Bioorg. Med. Chem. Lett. 44 (2021) 128108

Contents lists available at ScienceDirect

Bioorganic & Medicinal Chemistry Letters

journal homepage: www.elsevier.com/locate/bmcl

Development of BET inhibitors as potential treatments for cancer: A search for structural diversity

Matthew D. Hill *, Haiquan Fang, John Tokarski, Carolynn Fanslau, Zuzana Haarhoff, Christine Huang, Melissa Kramer, Krista Menard, Laura Monereau, John Morrison, Asoka Ranasinghe, Eric E. Shields, Ching Kim Tye, Richard Westhouse, Gerry Everlof, Steven Sheriff, Chunhong Yan, Frank Marsilio, Lisa Zhang, Tatyana Zvyaga, Francis Lee, Ashvinikumar V. Gavai, Andrew P. Degnan

Bristol Myers Squibb Research and Development, 100 Binney St, Cambridge, MA 02142-1096, USA

ARTICLE INFO

Keywords:
Bromodomain
BET
Cancer
Multiple myeloma
Lipophilic ligand efficiency

ABSTRACT

We describe our efforts to identify structurally diverse leads in the triazole-containing N1-carboline series of bromodomain and extra-terminal inhibitors. Replacement of the N5 "cap" phenyl moiety with various heteroaryls, coupled with additional modifications to the carboline core, provided analogs with similar potency, improved pharmacokinetic properties, and increased solubility compared to our backup lead, BMS-986225 (**2**). Rapid SAR exploration was enabled by a convergent, synthetic route. These efforts provided a potent BET inhibitor, 3-fluoropyridyl **12**, that demonstrated robust efficacy in a multiple myeloma mouse tumor model at 1 mg/kg.

Bromodomain and extra-terminal (BET) inhibition has gained considerable interest due to its ability to inhibit the master transcription factor c-Myc, which has been broadly implicated in cancer biology.[1] BET-family bromodomain-containing proteins[2] (BRD2, BRD3, BRD4, and BRDT) each have two binding domains (BD1 and BD2) that recognize acetylated lysine residues on histone tails.[3] As BET proteins bind to these modified histones, they facilitate gene expression by modulating chromatin architecture and recruiting transcriptional regulators to enhancer regions.[4] Small-molecule BET inhibitors can disrupt these enhancer-activator interactions to prevent transcription – an effect that is amplified in the context of superenhancers. Cancers caused by superenhancer-mediated *MYC* expression are hypersensitive to changes in factor concentration, which provides potential clinical opportunity for BET inhibition.[1b,5]

Early work in the field provided a structurally homogenous body of inhibitors like JQ1[1b] and GSK525762[6] (I-BET762, Fig. 1). Since that time, several second-generation BET inhibitors that employ novel chemical scaffolds, such as ABBV-075[7] and BMS-986158 (**1**),[8] have advanced into clinical trials for the treatment of hematologic malignancies and solid tumors. While utility in cancer has been the primary focus of BET inhibitors in clinical development, the scope of interest has also expanded beyond cancer, with preclinical efficacy reported in HIV, inflammation, acute heart failure, and other diseases.[9] (Fig. 2).

In an earlier disclosure, we described the discovery of N1-carboline **1**, a compound currently in phase I/IIa trials for advanced solid tumors.[8] In preclinical models, this lead was tolerated at efficacious doses and had suitable projected human pharmacokinetics (PK). After identification of clinical lead **1**, we initiated work toward the identification of a backup candidate using a three-pronged approach: 1) reduce clearance of the carboline series, 2) introduce structural diversity, and 3) improve physicochemical properties. In the first disclosure describing our backup efforts, we detailed work to reduce clearance using simple carboline core substitutions and by harnessing the kinetic isotope effect (Scheme 2) to identify BMS-986225 (**2**)[10] (Table 1) – a compound with increased liver microsome (LM) metabolic stability (metstab) and reduced glucuronidation and efflux potential. While these findings suggested the ability to increase total drug exposure, they did little to enhance solubility or reduce protein binding. Herein, we report our work to identify structurally diverse backup leads with increased solubility[11] and reduced human serum protein binding (PB)[12] without compromising the overall PK profile of backup **2**.[13]

To this end, we sought to replace the lipophilic phenyl of the "cap"

* Corresponding author.
E-mail address: matthew.hill@bms.com (M.D. Hill).

https://doi.org/10.1016/j.bmcl.2021.128108
Received 12 March 2021; Received in revised form 5 May 2021; Accepted 9 May 2021
Available online 13 May 2021

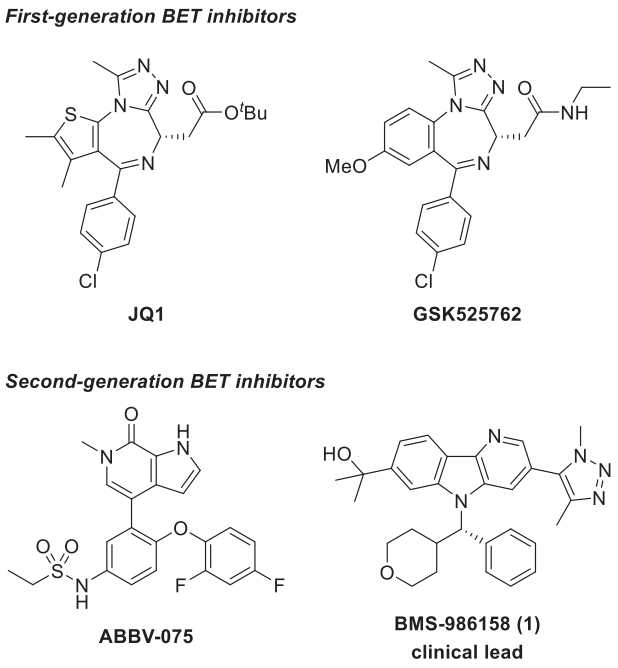

Fig. 1. Representative BET inhibitors.

with more polar heterocycles. Carboline analogs with "heteroaryl caps" were conveniently prepared using a previously reported convergent route.[8,10] The organomagnesium reagents used for all compounds discussed herein were prepared from 4-bromotetrahydropyran and magnesium, using iodine as an activating agent (Scheme 1). This Grignard reagent was subsequently added to various heteroaryl aldehydes in chilled tetrahydrofuran to afford racemic, secondary alcohols. To expedite preliminary SAR investigation, racemic alcohols were often used directly in the subsequent Mitsunobu step. Chiral resolution of final, racemic compounds using HPLC or SFC provided individual enantiomers for assay characterization. When resynthesis of final analogs was necessary or when specific caps were utilized for multiple final compounds, we found chiral resolution following Grignard addition to be most efficient.

Data for selected analogs are shown in Table 1.[14] We began with simple, 5-membered heteroaryl analogs like racemic 1,2,3-triazole **3**. Despite modest activity of **3** in a BRD4 binding assay (IC_{50} = 27 nM), a c-Myc functional assay that measured *MYC* expression (IC_{50} = 210 nM), and a Velcade®-resistant multiple myeloma (MM) cell proliferation assay (JJN3R IC_{50} = 710 nM), lipophilic ligand efficiency (LLE, calculation based on MM proliferation IC_{50})[15] was similar to highly potent backup **2** (LLE = 3.6 vs 3.7). Additional profiling revealed limited permeability (PAMPA at pH 7.4 = 120 nm/*sec*)[16] for 1,2,3-triazole **3**, consistent with its high polar surface area (PSA = 120 Å).[17] Molecular modeling of **3** in BRD4 (domain 1) revealed a hydrophobic channel accessible by *N1* alkylation of the triazole. In order to avoid non-selective alkylation of triazole **3**, we opted to test this hypothesis by preparing 1,2-pyrazole **4**. The methyl substituent of homochiral pyrazole **4** accessed the putative hydrophobic channel, which provided approximately twelve-fold improved binding over **3** (IC_{50} = 2.3 nM vs 27 nM), as well as improved activity in our c-Myc functional (IC_{50} = 7.1 nM vs 210 nM) and MM prolif. assays (IC_{50} = 55 nM vs 710 nM). Due to increased polarity of **4** relative to lead **2**, this compound had higher LLE (4.4 vs 3.7) and improved LM metstab across species.[18] Conversely, this increased polarity (PSA = 96 Å) led to limited permeability (PAMPA at pH 7.4 = 150 nm/*sec*) that eroded translation of BRD4 binding to cell-based functional and prolif. activity compared to our leads. For example, the MM proliferation to BRD4 binding IC_{50} ratio for backup lead **2** was 6.7, whereas the ratio for pyrazole **4** was 23.9.

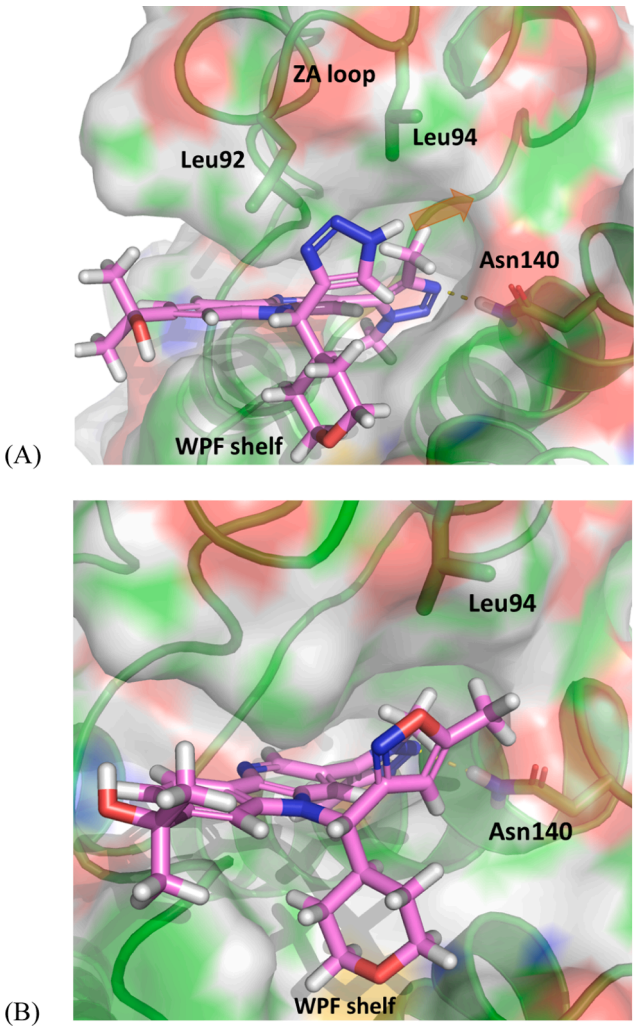

Fig. 2. A) Modeling suggested an opportunity to improve potency of 1,2,3-triazole 3, in BRD4 (domain 1). Carbons of 3 are colored magenta. Hydrogen bonds are shown as yellow dashes. B) Model of optimized isoxazole 5 in BRD4 (domain 1).

Though isoxazole **5** was not expected to be highly permeable (PSA = 104 Å), this analog was designed to mitigate possible steric interactions between the N1 methyl of pyrazole **4** and the ZA loop of the binding site. As anticipated, this change led to increased potencies across our *in vitro* assays (e.g. MM prolif. IC_{50} = 11 nM, LLE = 4.8); however, diminished LM metstab, especially in mouse (ms), prevented advancement of **5**, given the preclinical importance of this species. In prior studies, we replaced the C4′-Tz Me with Me-d_3 to reduce clearance (Scheme 2).[10] Comparison of isoxazole **5** (msLM T½ = 10 min) with Me-d_3, isoxazole **6** (msLM T½ = 30 min) confirmed similar effects with heteroaryl caps. Free fraction was quite high for **6** (hPB = 14% free) relative to backup **2** (hPB = 1% free), but this polarity-driven effect was accompanied by limited permeability (PAMPA at pH 7.4 = 260 nm/*sec*). Prior efforts revealed significant fluoro-derived influence on permeability.[10,19] Learning from this work, we prepared fluoro derivatives **7**–**9**. Fluoro substituents at C6, C8, and C9 all improved permeability, but the effects varied considerably (C6 > C8 > C9).

Significantly, C6-fluoroisoxazole **7** demonstrated improved solubility in a 50 mM phosphate buffer at pH 6.5 (120 μg/mL) relative to backup **2** (4 μg/mL)[20] and improved hPB % free (16% vs 1%, respectively). Following a 24 h mouse PK study (3 mg/kg, PO: AUC_{24h} = 8.7 μM*h), we advanced **7** into a MM mouse xenograft tumor model (JJN3R).[21] In this experiment, designed to recapitulate human tumor

Table 1
BRD4 and c-Myc inhibition, MM (JJN3R) proliferation, LLE, metstab, PAMPA, and PB data.

Compound		BRD4 IC_{50} ± SEM (nM)[a]	c-Myc IC_{50} ± SEM (nM)[a]	MM prolif. IC_{50} ± SEM (nM)[a]	LLE[b]	metstab T½ (min)(h/r/ms/d/mk)[c,d]	PAMPA pH 7.4 (nm/*sec*)	PB % free(h)
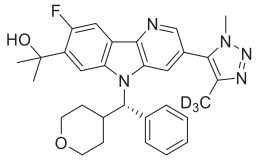	**2**	0.9 ± 0.2 (6)	2.0 ± 1.0 (7)	6.0 ± 1.0 (8)	3.7	52/46/41/32/19	690	1
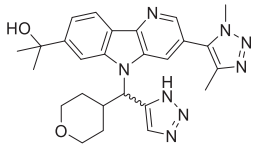	**3**	27 ± 13 (2)	210 (1)	710 (1)	3.6	na	120	na
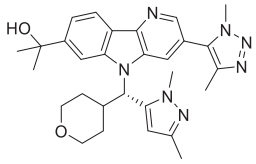	**4**	2.3 ± 0.8 (2)	7.1 ± 1.0 (3)	55 ± 23 (3)	4.4	83/59/50/52/36	150	na
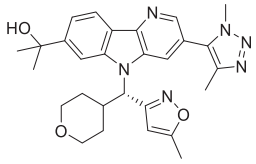	**5**	1.6 ± 0.2 (3)	2.8 ± 0.3 (3)	11 ± 6 (4)	4.8	61/26/10/38/16	350	na
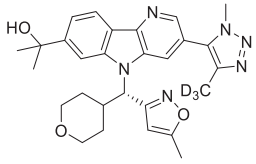	**6**	1.2 (1)	2.1 ± 0.3 (2)	9.9 ± 1.1 (3)	4.9	64/33/30/75/37	260	14
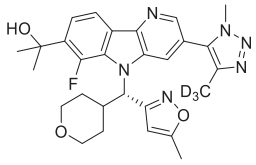	**7**	2.0 ± 1.2 (3)	3.9 ± 1.4 (3)	13 ± 4 (3)	4.6	79/30/30/52/23	800	16
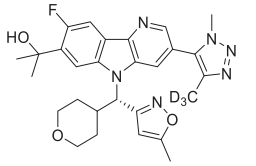	**8**	1.4 (1)	2.2 ± 0.6 (3)	14 ± 4 (3)	4.6	54/3/26/33/21	690	na
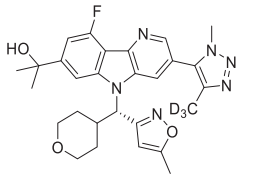	**9**	na	2.8 ± 0.2 (3)	3.9 ± 3.0 (3)	5.2	120/33/17/71/34	410	na
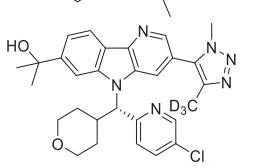	**10**	1.0 ± 0.2 (8)	1.2 ± 0.2 (4)	4.8 ± 1.6 (4)	4.3	55/62/35/61/37	610	6
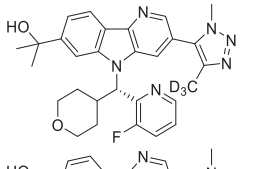	**11**	0.9 ± 0.2 (5)	1.0 ± 0.2 (3)	3.6 ± 0.8 (3)	4.9	79/48/24/36/22	270	4
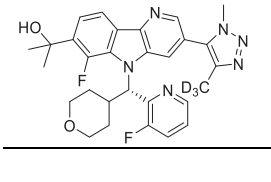	**12**	0.6 ± 0.3 (4)	0.9 ± 0.3 (4)	1.7 ± 0.2 (3)	5.1	75/47/16/37/22	420	6

[a] Number of determinations in parentheses. [b]LLE = pIC50 − cLogP. [c]human = h, rat = r, mouse = ms, dog = d, monkey = mk. [d]Measurement limit = 120 min.

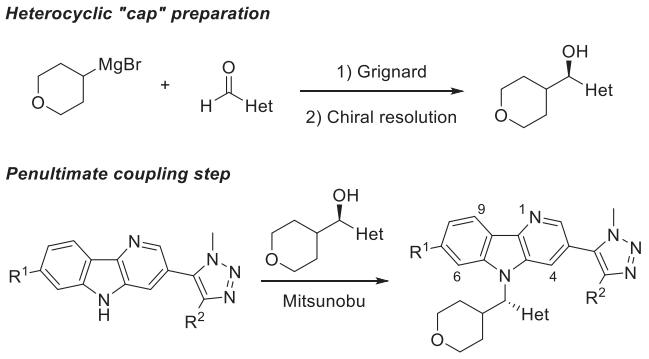

Scheme 1. Highlighted steps en route to carbolines with heteroaryl N5 caps.

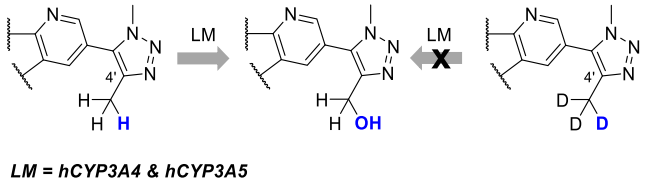

Scheme 2. Deuteration strategy to mitigate primary route of metabolism.

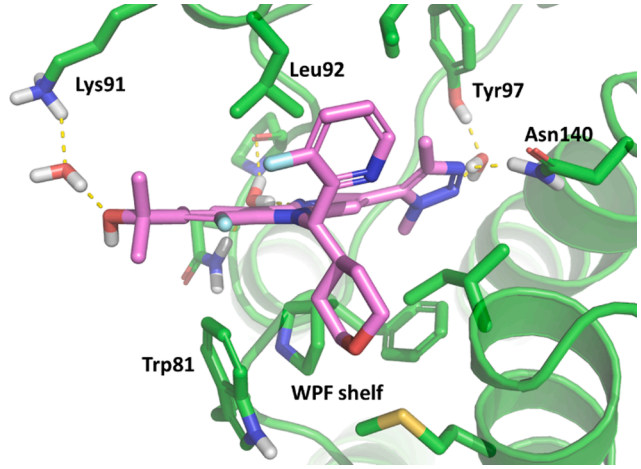

Fig. 3. X-ray structure of BRD4 (domain 1) bound to 12. Close-up image of interactions of 12 with BRD4 and waters. Some of the waters directly hydrogen bound to 12 are shown.

physiology, mice were dosed (PO, QD) for 7 days beginning 8 days after tumor-cell implantation. C6-Fluoroisoxazole **7** treatment marginally impaired the growth of established MM tumors (TGI = 71%) at MED = 4 mg/kg; the response was more robust with backup **2** (TGI = 77% at 2 mg/kg). Based on these data, we set new cellular potency guidelines for moving analogs into efficacy studies (e.g. JJN3R prolif. IC_{50} < 10 nM).

After extensive SAR investigation of 5-membered, heteroaryl compounds, we shifted focus to 6-membered heteroaryls. Empirically, we found analogs that incorporated the phenyl cap could achieve single-digit nM potencies in our MM assay.[8,10] Therefore, we prepared pyridine and diazine derivatives with varied substitution and found halo-containing 2-pyridyl analogs were most potent across binding and cell-based assays. 5-Chloropyridyl **10** and 3-fluoropyridyl **11** were both <5 nM in our MM prolif. assay (LLE > 4.3) with improved or equivalent metstab and hPB relative to our leads. Although the permeability of 5-

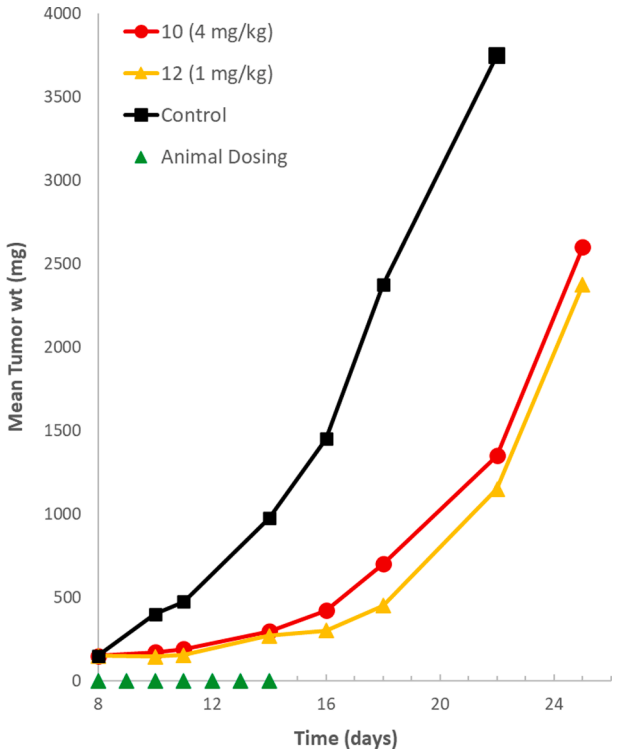

Fig. 4. Activity of leads in JJN3R MM tumor model.

chloropyridyl **10** (PAMPA at pH 7.4 = 610 nm/*sec*) was well above our acceptable threshold (PAMPA at pH 7.4 > 400 nm/*sec*), permeability was limited for 3-fluoropyridyl **11** (PAMPA at pH 7.4 = 270 nm/*sec*).[22] Fortunately, installation of a C6-fluoro substituent on the carboline provided improved permeability for analog **12** (PAMPA at pH 7.4 = 420 nm/*sec*), although to a lesser extent than had been observed with 5-membered heteroaryl caps (**11** → **12** = 56% increase vs **6** → **7** = 210% increase). 3-Fluoropyridyl **12** was exquisitely potent across our *in vitro* assays (e.g. MM prolif. IC_{50} = 1.7 nM, LLE = 5.1) due to binding interactions that included several conserved water residues (Fig. 3).[8] The overall metstab profile was superior to backup **2** except for msLM (msLM T½ = 16 min vs 41 min, respectively). Despite the 61% decrease in msLM T½ between backup **2** and **12**, we observed only 13% decreased exposure (3 mg/kg, PO: AUC_{24h} = 12.6 and 10.9 μM*h, respectively) in 24 h mouse PK study. Gratifyingly, **12** was highly soluble in 50 mM phosphate buffer at pH 6.5 (91 μg/mL) and provided increased free fraction (hPB = 6% free) relative to earlier leads.

Due to their robust antiproliferative effects in the JJN3R cell line, both pyridyl analogs **10** and **12** advanced into the MM mouse tumor model (JJN3R). Mice were dosed (PO, QD) for 7 days beginning 8 days following tumor-cell implantation (Fig. 4). Treatment with **12** impaired tumor growth (TGI = 91%) at MED = 1 mg/kg and demonstrated more robust efficacy than a 4 mg/kg dose (TGI = 78%) of backup **2**.[23] Compared to **2**, 5-Chloropyridyl **10** was similarly efficacious (TGI = 76%) at a 4 mg/kg dose.

In summary, we explored heteroaryl cap SAR to introduce structural diversity and improve physicochemical properties of backup compounds. We began looking at 5-membered heteroaryl caps and used structural information to improve *in vitro* potency (~70 fold). From these efforts, C6-fluoroisoxazole **7** was identified. This compound had reduced human serum protein binding, improved solubility, and increased exposure in a mouse PK study. In a MM mouse tumor model, **7** provided only modest efficacy, a result attributed to >10 nM potency in

the same MM cell line. This result inspired an SAR shift to 6-membered heteroaryl caps, including 2-pyridyl analogs **10** and **12**. Both pyridyl derivatives provided enhanced exposure in mouse PK and were <5 nM in our MM cell proliferation assay, which translated to robust *in vivo* efficacy when compared to our backup lead, BMS-986225 (**2**). 3-Fluoropyridyl **12** also met our goals of improved solubility and free fraction in hPB. Additional optimization studies will be reported in due course.

Declaration of Competing Interest

The authors declare that they have no known competing financial interests or personal relationships that could have appeared to influence the work reported in this paper.

Acknowledgements

We thank Chiradeep Panja, Premsai Neithnadka, Manivel Pitchai, Subhabrata Chaudhury, and Ananta Karmakar for large-scale preparation of chemical intermediates.

Appendix A. Supplementary data

Supplementary data to this article can be found online at https://doi.org/10.1016/j.bmcl.2021.128108.

References

1 (a) Whitfield JR, Beaulieu ME, Soucek L. Front. Cell Dev. Biol. 2017; 5; 1. (b) Delmore JE, Issa GC, Lemieux ME, et al. Cell 2011; 146; 904.
2 (a) Prinjha RK, Witherington J, Lee K. Trends Pharma-col. Sci. 2012; 33; 146; (b) Chung CW. Prog. Med. Chem. 2012; 51; 1; (c) Fu LL, Tian M, Li X, et al. Oncotarget 2015; 6; 5501.
3 Choudhary C, Kumar C, Gnad F, et al. *Science.* 2009;325:834.
4 (a) Patel JH, Du Y, Ard PG, et al., Mol. Cell Biol. 2004; 24; 10826; (b) MYC transcription has been linked to high levels of lysine acetylation: Martile MD, Bufalo DD, Trisciuoglio D. Oncotarget 2016; 7; 55789.
5 Lovén J, Hoke HA, Lin CY, et al. *Cell.* 2013;153:320.
6 Mirguet O, Gosmini R, Toum J, et al. *J. Med. Chem.* 2013;56:7501.
7 McDaniel KF, Wang L, Soltwedel T, et al. *J. Med. Chem.* 2017;60:8369.
8 Gavai AV, Norris D, Tortolani D, et al. Discovery of Clinical Candidate BMS-986158, an Oral BET Inhibitor, for the Treatment of Cancer. *Cancer Res.* 2018;13.
9 (a) Ferri E, Petosa C, McKenna CE. Biochem. Pharmacol. 2016; 106; 1; (b) Romero FA, Taylor AM, Crawford TD, Tsui V, Côté A, Magnuson S. J. Med. Chem. 2016; 59; 1271; (c) Liu Z, Wang P, Chen H, Wold EA, Tian B, Brasier AR, Zhou J. J. Med. Chem. 2017; 60; 4533.
10 Hill M, Fang H, Norris D, et al., Discovery of potent BET inhibitors as potential treatments for cancer. ACS Division of Medicinal Chemistry Scientific Abstracts for the 256th Meeting and Exposition 2018; 256: Abstract 265.
11 Di L, Fish PV, Mano T. *Drug Discov. Today*. 2012;17:486.
12 Liu X, Wright M, Hop CECA. *J. Med. Chem.* 2014;57:8234.
13 Metabolic softs pots varied between species.
14 See Supplemental Material for experimental details.
15 Hopkins AL, Keseru GM, Leeson PD, Rees DC, Reynolds CH. *Nat. Rev.* 2014;13:105.
16 Parallel Artificial Membrane Permeability Assay = PAMPA.
17 Artursson P, Bergström CAS. *Intestinal Absorption: The Role of Polar Surface Area.* In *Drug Bioavailability: Estimation of Solubility, Permeability. Absorption and Bioavailability; Wiley-VCH Verlag GmbH & Co. KgaA.* 2003;339.
18 St. Jean Jr. DJ, Fotsch, C. J. Med. Chem. 2012; 55; 6002..
19 Gillis EP, Eastman KJ, Hill MD, Donnelly DJ, Meanwell NA. *J. Med. Chem.* 2015;58:8315.
20 Solubility of 7 was measured using CH3 isotope.
21 Rossi M, Botta C, Arbitrio M, Grembiale RD, Tagliaferri P, Tassone P. *Oncotarget.* 2018;9:20119.
22 Permeability was independent of halopyridine regioisomerism.
23 Efficacy for backup 2 was measured in a separate but identical study.